NASA/TM—2014-216630

Test Methodology Development for Experimental Structural Assessment of ASC Planar Spring Material for Long-Term Durability

Gunjin Yun, A.B.M. Abdullah, and Wieslaw Binienda
University of Akron, Akron, Ohio

David L. Krause
Glenn Research Center, Cleveland, Ohio

Sreeramesh Kalluri
Ohio Aerospace Institute, Brook Park, Ohio

February 2014

NASA STI Program . . . in Profile

Since its founding, NASA has been dedicated to the advancement of aeronautics and space science. The NASA Scientific and Technical Information (STI) program plays a key part in helping NASA maintain this important role.

The NASA STI Program operates under the auspices of the Agency Chief Information Officer. It collects, organizes, provides for archiving, and disseminates NASA's STI. The NASA STI program provides access to the NASA Aeronautics and Space Database and its public interface, the NASA Technical Reports Server, thus providing one of the largest collections of aeronautical and space science STI in the world. Results are published in both non-NASA channels and by NASA in the NASA STI Report Series, which includes the following report types:

- TECHNICAL PUBLICATION. Reports of completed research or a major significant phase of research that present the results of NASA programs and include extensive data or theoretical analysis. Includes compilations of significant scientific and technical data and information deemed to be of continuing reference value. NASA counterpart of peer-reviewed formal professional papers but has less stringent limitations on manuscript length and extent of graphic presentations.

- TECHNICAL MEMORANDUM. Scientific and technical findings that are preliminary or of specialized interest, e.g., quick release reports, working papers, and bibliographies that contain minimal annotation. Does not contain extensive analysis.

- CONTRACTOR REPORT. Scientific and technical findings by NASA-sponsored contractors and grantees.

- CONFERENCE PUBLICATION. Collected papers from scientific and technical conferences, symposia, seminars, or other meetings sponsored or cosponsored by NASA.

- SPECIAL PUBLICATION. Scientific, technical, or historical information from NASA programs, projects, and missions, often concerned with subjects having substantial public interest.

- TECHNICAL TRANSLATION. English-language translations of foreign scientific and technical material pertinent to NASA's mission.

Specialized services also include creating custom thesauri, building customized databases, organizing and publishing research results.

For more information about the NASA STI program, see the following:

- Access the NASA STI program home page at *http://www.sti.nasa.gov*

- E-mail your question to *help@sti.nasa.gov*

- Fax your question to the NASA STI Information Desk at 443–757–5803

- Phone the NASA STI Information Desk at 443–757–5802

- Write to:
  STI Information Desk
  NASA Center for AeroSpace Information
  7115 Standard Drive
  Hanover, MD 21076–1320

NASA/TM—2014-216630

Test Methodology Development for Experimental Structural Assessment of ASC Planar Spring Material for Long-Term Durability

Gunjin Yun, A.B.M. Abdullah, and Wieslaw Binienda
University of Akron, Akron, Ohio

David L. Krause
Glenn Research Center, Cleveland, Ohio

Sreeramesh Kalluri
Ohio Aerospace Institute, Brook Park, Ohio

National Aeronautics and
Space Administration

Glenn Research Center
Cleveland, Ohio 44135

February 2014

Acknowledgments

The authors appreciate the inspiring leadership and management at NASA Glenn Research Center provided by Dick Shaltens, Wayne Wong, Jeff Schreiber, Lanny Thieme, Scott Wilson, and Geoff Bruder, as well as the full support and technical management of Drs. Ajay Misra and Steven Arnold. The authors thank Ralph Pawlik and Frank Bremenour for their expert experimental advice and technical collaboration. The authors truly appreciate the efforts and cooperation enjoyed from Sunpower, including the professional work of Kyle Wilson, Doug Mansfield, Courtney Lenart, and their consultant Barry Penswick. The authors also would like to thank Mr. Brett Bell, Mr. William Wenzel, and Mr. Dale Ertley (all from the College of Engineering, the University of Akron) for their strong support in manufacturing and machining of materials. The Science Mission Directorate at NASA Headquarters provided funding to complete the work described herein, and the authors truly are grateful for that enduring commitment.

Level of Review: This material has been technically reviewed by technical management.

Available from

NASA Center for Aerospace Information
7115 Standard Drive
Hanover, MD 21076–1320

National Technical Information Service
5301 Shawnee Road
Alexandria, VA 22312

Available electronically at http://www.sti.nasa.gov

Test Methodology Development for Experimental Structural Assessment of ASC Planar Spring Material for Long-Term Durability

Gunjin Yun, A.B.M. Abdullah, and Wieslaw Binienda
University of Akron
Akron, Ohio 44325

David L. Krause
National Aeronautics and Space Administration
Glenn Research Center
Cleveland, Ohio 44135

Sreeramesh Kalluri
Ohio Aerospace Institute
Brook Park, Ohio 44142

Abstract

A vibration-based testing methodology has been developed that will assess fatigue behavior of the metallic material of construction for the Advanced Stirling Convertor displacer (planar) spring component. To minimize the testing duration, the test setup is designed for base-excitation of a multiple-specimen arrangement, driven in a high-frequency resonant mode; this allows completion of fatigue testing in an accelerated period. A high performance electro-dynamic exciter (shaker) is used to generate harmonic oscillation of cantilever beam specimens, which are clasped on the shaker armature with specially-designed clamp fixtures. The shaker operates in closed-loop control with dynamic specimen response feedback provided by a scanning laser vibrometer. A test coordinator function synchronizes the shaker controller and the laser vibrometer to complete the closed-loop scheme. The test coordinator also monitors structural health of the test specimens throughout the test period, recognizing any change in specimen dynamic behavior. As this may be due to fatigue crack initiation, the test coordinator terminates test progression and then acquires test data in an orderly manner. Design of the specimen and fixture geometry was completed by finite element analysis such that peak stress does not occur at the clamping fixture attachment points. Experimental stress evaluation was conducted to verify the specimen stress predictions. A successful application of the experimental methodology was demonstrated by validation tests with carbon steel specimens subjected to fully-reversed bending stress; high-cycle fatigue failures were induced in such specimens using higher-than-prototypical stresses.

1.0 Introduction

The National Aeronautics and Space Administration (NASA) Glenn Research Center (GRC), Cleveland, Ohio provides life and reliability verification and advanced technology development for the Advanced Stirling Convertor (ASC) project. Sunpower, Athens, Ohio is developing the ASC under a NASA Research Announcement award. The ASC is a mechanism that converts the heat of decay from a General Purpose Heat Source into electrical power. It is proposed for use in the high-efficiency Advanced Stirling Radioisotope Generator (ASRG) being developed by Lockheed Martin, Valley Forge, Pennsylvania, and is identified as a promising power source for future long duration scientific space missions. More information about the ASC and ASRG projects is available in References 1 to 3. The work presented herein supports the experimental structural assessment of ASC Displacer (planar) Spring material for long-term durability. The ASC planar spring provides translational stiffness and the

corresponding spring rate for oscillation of the displacer component. This spring design uses geometry, materials, and fabrication processes in unique ways that require fatigue testing of the material of construction to accurately assess the part's structural life. Accelerated component-level testing of the planar spring is being performed at Sunpower to help validate design life by the extrapolation of high stress, low cycle count test results to the low stress, high cycle count design conditions. The planar spring life assessment requires further testing in the giga-cycle fatigue (GCF) range to verify and properly evaluate the processed material's durability for the long-term life requirement of tens of billions of low stress cycles without degradation. This testing must be performed at prototypical and near-prototypical stress levels, and at high frequencies to assure that test results are available within a reasonable time period. The objective of this work was to develop a GCF test procedure, geometric designs of test specimens and fixtures, test controls, and instrumentation, to assure that valid experimental data can be obtained from specimens fabricated from actual planar spring material and using planar spring processing techniques in future testing. This effort included validation that the test method permits stable operation of an electro-dynamic exciter in closed-loop control.

In this effort, experimental development of a closed-loop GCF test configuration for multiple specimens was emphasized. This resonance fatigue test mechanism was synchronized by a GCF Test Coordinator. Substantial change in dynamic responses, such as resonant frequency or other damage sensitive indices, imply stiffness changes associated with fatigue crack initiation and propagation. With the closed-loop control technique, re-tuning the excitation frequency to the shifted resonant frequency of specimen was accomplished, and thus by tracking preset phase angle and frequency change monitored by the GCF Test Coordinator, satisfactory control of the test over the fatigue crack propagation period was attained.

2.0 Equipment for Closed-Loop GCF Testing

The GCF test configuration includes the following components.

1. Polytec Scanning Vibrometer (PSV), Model PSV-400-M2-20, from Polytec, Inc. (Fig. 1) is a scanning laser vibrometer (SLV) system (Refs. 4 to 7) which includes the following modules:
   a. *Junction Box, PSV-E-400*: The junction box is an interface between the laser scanning head, the controller, and the data management system PC. It has four available ICP-compatible analog input channels: one channel is used for an accelerometer attached to the shaker armature; another is used for velocity data from the OFV-5000 controller. An auxiliary output of the digital I/O port sends high and low TTL signals to the Data Physics (DP) ABACUS chassis to activate programmed functions on the DP shaker system.
   b. *Controller, OFV-5000*: The vibrometer controller has standard BNC connectors to send velocity data in analog voltage signals to the control channel of the DP ABACUS chassis and the junction box. The controller can measure up to 10 m/sec (33 ft/sec) velocity.
   c. *Data Management System PC, PSV-W-400*: This is a desktop PC for accessing measured data using PSV vibrometer software.
   d. *Scanning Head, PSV-I-400*: The scanning head is a long-range laser scanning unit which is installed on a stable tripod. It is positioned at an optimum stand-off distance, approximately 500 mm (20 in.) from the front face of the head to the specimen.

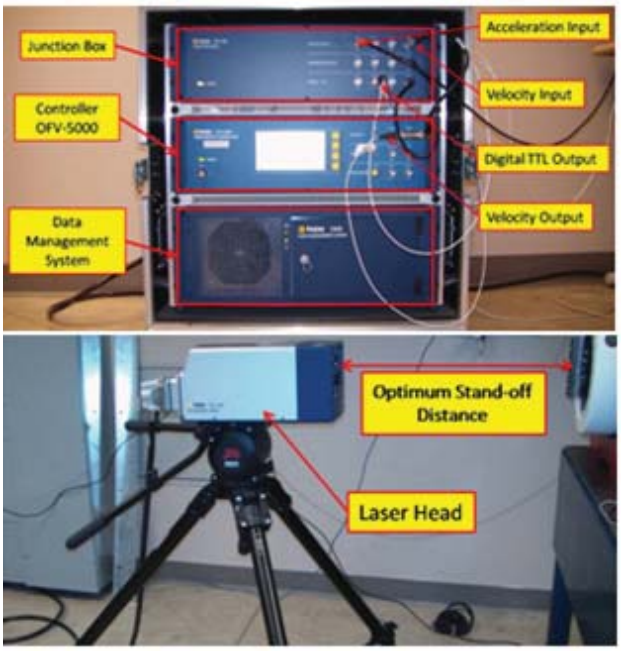

Figure 1.—PSV-400-M2-20 system.

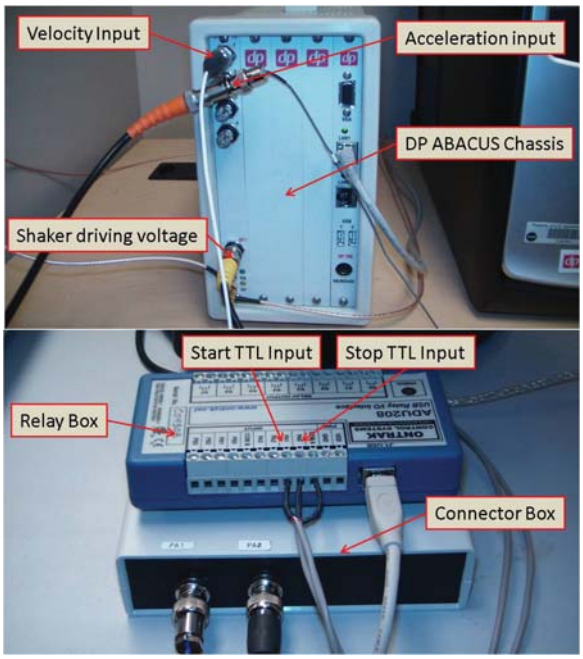

Figure 2.—DP ABACUS chassis and relay box.

2. SignalStar Vector Vibration/Shaker Controller System, from DP (Ref. 8), which includes the following components (Fig. 2):

   a. *ABACUS Chassis*: The chassis has four standard BNC input channels: one is connected to the OFV-5000 controller for acquiring velocity data from the specimens; another channel is connected to the accelerometer installed on the shaker armature. The accelerometer is also connected to the reference channel of the PSV junction box.
   b. *Relay Box, ONTRAK ADU 208*: The relay box physically interfaces system I/0 signals; it connects the OFV-5000 controller to the desktop PC through a USB cable, and it transmits digital TTL signals to coordinate dwell testing when multiple specimens are used.
   c. *Desk Top PC and Monitor*: A Windows XP desktop computer runs the DP SignalStar Vector software for vibration control, and it is connected to the DP ABACUS chassis through TCP/IP.

3. SignalForce Electrodynamic Shaker System, from DP (Ref. 9), which includes the following components (Fig. 3):

   a. *Shaker, V100/DSA1-1K*: This air-cooled electro-dynamic exciter (shaker) has a maximum sine force capability of 1000 N (225 lbs) and maximum acceleration of 1225 m/s^2 (125 g). The moving armature mass is 0.8 kg (1.7 lbs). Its frequency range is from DC to 7000 Hz, with an armature resonant frequency at 6850 Hz. It is connected to the field supply unit.
   b. *Power Amplifier, SS1000T*: The amplifier is connected to the field supply unit for power acquisition and to the ABACUS chassis for shaker driving voltage.
   c. *Field Supply Unit, FSU100*: The field supply unit provides power to the amplifier and shaker.
   d. *Cooling Blower Unit*: A flux jet cooling blower unit is connected to the V100 shaker to lower the operating temperature during long-term use.

4. External Hard Drive, 1TB Element, from Western Digital: The hard drive is connected to the PC to save GCF test data (specimen velocity data, Frequency Response Function (FRF) and the number of cycles for each scanning point, displacement, etc.).

Figure 3.—DP shaker system.

Figure 4.—Facility upgrade for GCF testing.

5. Accelerometer, 3030B, from Dytran Instruments, Inc. (Ref. 10): The accelerometer is installed on the shaker armature to provide reference acceleration data; the signal is sent to both the DP ABACUS chassis and the PSV system.

6. Strain Gage, WK-06-062AP-350, from Vishay Micro-Measurements, Inc. (Ref. 11): The WK series strain gage is made of fully encapsulated K-alloy with high endurance leads. The maximum strain range is ±1.5 percent. Resistance of strain gages is 350±0.3 percent Ω.

7. Signal Conditioning Unit, NI-1520; Strain Gage Termination Block, NI-1314; chassis module, NI SCXI-1001; M Series DAQ Board, PXI-6259; chassis module, PXI 1042, all from National Instrument (NI) Inc.: The strain gage signal conditioning equipment is used during calibration testing for stress evaluation.

8. Network Camera, BL-C1A, from Panasonic: A network camera is installed for remote surveillance of shaker operations.

9. Function Generator, 33250A, from Agilent Technologies, Inc.: Shaker driving voltage signals are generated from an external waveform function generator.

10. Other laboratory facilities: For a secure testing environment, a permanent wall was built as shown in Figure 4. In addition, laboratory electric power was upgraded to accommodate the larger power consumption of the shaker system.

11. Software, GCF Test Coordinator: For closed-loop GCF testing, a unique automated testing coordinator was developed. Its features are explained in Section 5.0.

12. Software, Data Physics SignalStar Vector: The main use of this software is a feature that enables feedback-controlled resonant fatigue testing.

3.0 Shaker Evaluation

Along with specimen design and system damping, the maximum attainable amplitudes of the DP V100 shaker armature are important values that determine the maximum stress level attainable in the specimen. One of the goals in shaker evaluation was to determine if it had sufficient power to reach the targeted stress levels in the specimen to achieve fatigue failures within the requisite time frame.

The approximate weight of 10 specimens, each 64 mm (2.5 in.) long, combined with the fixture was 3.8 N (0.85 lb). Before the specimens and fixture were made, a circular dummy mass with comparable weight was manufactured, and the armature amplitudes were evaluated. The shaker was operated at different frequencies, and the armature displacement amplitudes (i.e., one half of the peak-to-peak displacements) were measured using the Polytec laser vibrometer. Figure 5 shows the dummy mass attached to the shaker, and Figure 6 shows 10 specimens properly mounted in the fixture, which is attached to the shaker.

An analytical equation was derived for the armature displacement amplitude based on energy conservation between electrical and mechanical kinetic energy. Small losses due to friction, generated heat, inherent damping in the mechanical system, and other losses, were neglected.

$$D_{0-pk}^{\max} = \frac{80\%\ \text{of Max Accl}_{0\text{-pk}} \times \sqrt{\dfrac{\text{Armature Mass}}{\text{Armature Mass} + \text{Mass of Specimen \& Fixture}}}}{4 \times \pi^2 \times \text{Excitation Frequency}^2} \tag{1}$$

As indicated in Equation (1), the displacement amplitude is dependent on mass of the armature, specimen and fixture, and operating frequency.

Analytically computed displacement amplitudes were compared with experimental values over the range of 200 to 2100 Hz as shown in Figure 7. It was observed that test results were in close agreement with the analytical estimation in this frequency range. However, as the operating frequency approached 6850 Hz for the V100 (not shown), it was observed that the displacement amplitude rapidly increases, diverging from analytical predictions. This was expected since the analytical estimation equation does not take into account dynamics of the shaker armature, which the manufacturer states has a first resonance at 6850 Hz. Utilization of the shaker resonance phenomenon was considered for the purpose of gaining higher specimen displacement amplitudes for the test specimens, but large displacement amplitudes at the shaker resonance frequency were inherently inconsistent. Thus, it was decided to not operate the shaker near its own resonant frequency.

Figure 5.—Dummy mass attached to shaker armature.

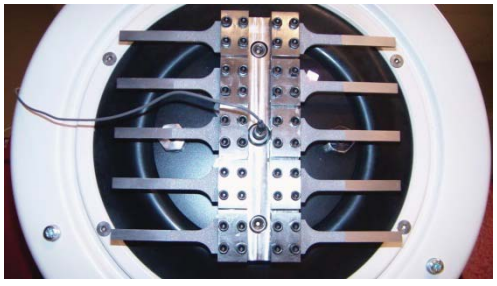

Figure 6.—Specimen and fixture for shaker evaluation.

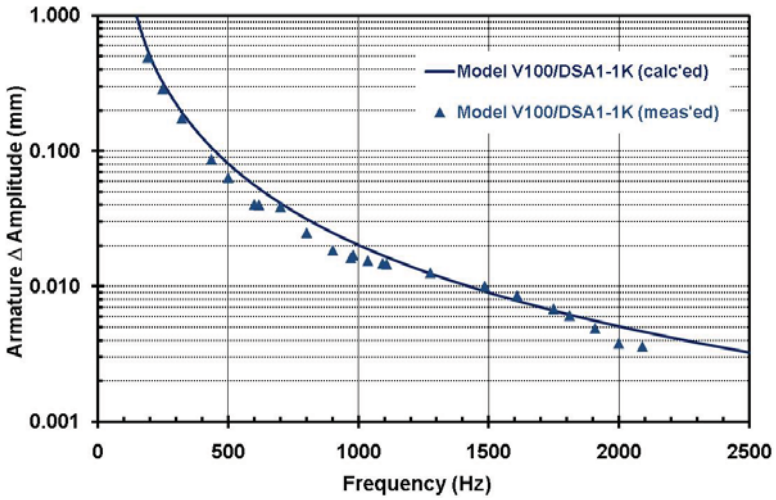

Figure 7.—Performance of shaker over an operating frequency range.

As discussed in the next section, the experimentally evaluated shaker amplitudes were used in subsequent three-dimensional (3D) finite element (FE) analyses to optimize the design of the specimen geometry, as well as to perform an evaluation of system damping.

4.0 Test Specimen Design and Fixtures

4.1 Design of the Test Specimen

Motivated by good response from 3D FE simulation using frequency analysis and direct solution steady-state dynamic analysis in ABAQUS (Dassault Systèmes) for different boundary conditions, the test specimen was designed as a cantilever. The geometric constraints included the specimen thickness, which was required to be approximately 1.8 mm (0.071 in.), and the gage area width at the location of maximum stress, which was required to be approximately 5 mm (0.2 in.). To avoid the possible occurrence of fretting fatigue or highly localized stress concentrations, it was desired to identify a specimen geometry that possessed a mode shape producing the maximum stress, greater than the endurance limit, away from the clamped edge. Another consideration was to minimize the testing period by designing the mode shape to be of reasonably high natural frequency but within the operating frequency range of shaker.

The original test plan was to shake the specimen near its second bending mode's natural frequency. However, it was found that the DP shaker could not produce the necessary armature displacements to achieve stresses larger than the endurance limit at the high second mode frequency for reasonably sized specimens. Therefore, the specimen's lower first bending mode natural frequency was used, which allowed the larger armature amplitudes necessary to reach the required higher stresses in the specimens.

A series of FE analyses were performed to optimize specimen geometry. The specimen base (the gripped zone area near the fixed end) was widened to reduce the stress level adjacent to the fixed boundary. Once optimized, a test matrix could be formed by varying the length of specimens, which results in different natural frequencies, shaking amplitudes, and consequently stress levels, and thus, distinct fatigue lives.

To explore the specimen design space, analyses were completed with several specimen configurations, including: added lumped mass at the tip of specimen; hourglass-shape specimen in which the section is reduced near the peak stress region; hourglass-shape specimens with a wider tip area; specimens with propped-cantilever boundary conditions; specimens with fixed-fixed boundary conditions; and, specimens with sharp notches in which high stress occurs in a constricted area. But, all these alternative designs resulted in localized stress concentrations.

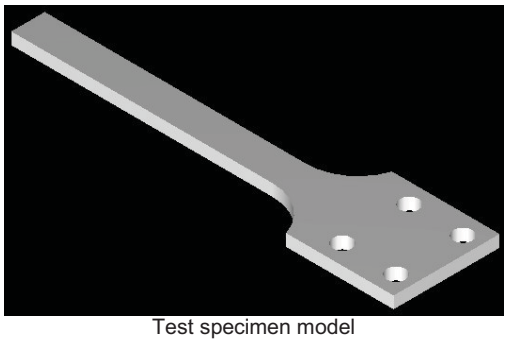

Test specimen model

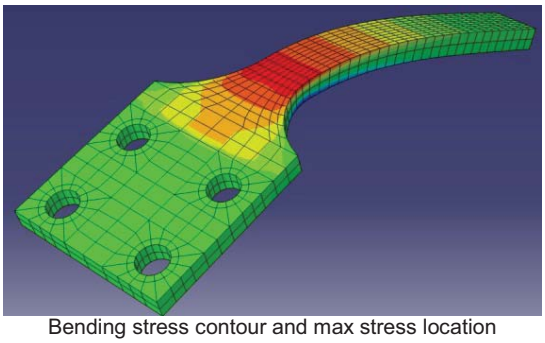

Bending stress contour and max stress location

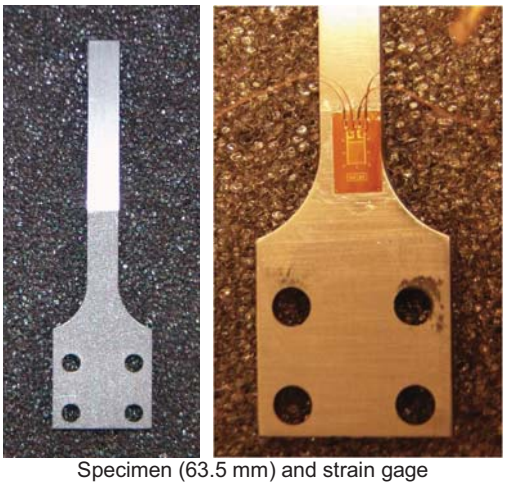

Specimen (63.5 mm) and strain gage

Figure 8.—Specimen and results of 3D FE analysis.

Finally, optimized specimen geometry was achieved as shown in Figure 8; the highest stress occurs at the end of the curvature between the base and the gage area, with a very slight stress concentration, similar to the ASC Displacer Spring design.

Scatter is an inherent characteristic of mechanical properties of structures and materials. This especially applies to fatigue properties. The fatigue test lives of similar specimens or structures under the same loading can be significantly different. Hence, a fixture block was designed to accommodate 10 specimens to facilitate testing multiple specimens simultaneously. Simultaneous testing of 10 specimens also reduces the total amount of testing time to obtain fatigue repeat data. One design constraint was to keep the fixture weight low, as more weight would demand more shaker power to excite the specimens. Figure 9 shows the designed geometric model as well as 10 manufactured specimens and the fixture. Detailed drawings for the specimen and fixtures are illustrated in Appendix A, Figures 27 to 30.

4.2 Evaluation of Damping

Damping had a significant influence on the attainable stress level. Damping was observed to be dependent on tip displacement amplitudes of the specimen, as tip displacements fell far short of initially expected values for the lower frequency, higher stress cases.

In 3D FE analyses, damping was modeled as structural damping; analyses were performed with varying values of damping so that the resulting calculated strains at the maximum stress location correlated to the measured experimental strains. In this way, an estimate of damping was obtained for various stress levels; these results are preliminary, particularly at high strain values, where testing indicated that yielding of at least some of the specimens occurred.

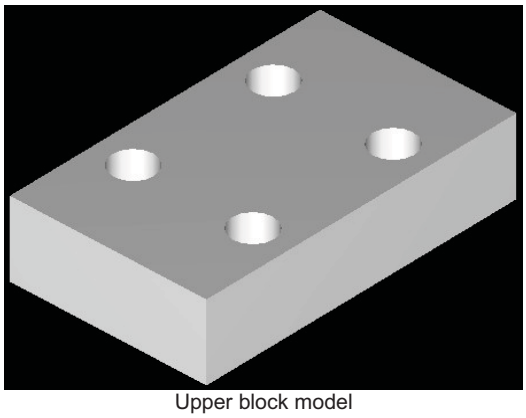

Upper block model

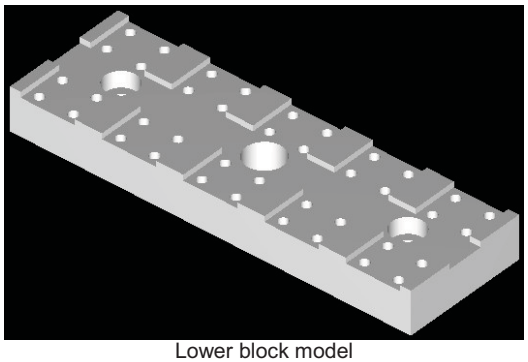

Lower block model

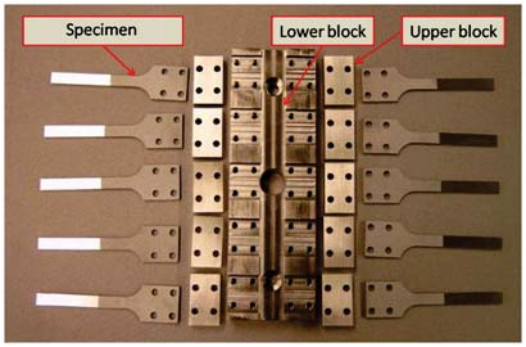

Manufactured parts

Figure 9.—Fixture and specimens.

5.0 Closed-Loop GCF Testing System

A closed-loop GCF testing system was developed by connecting two systems, the PSV Scanning Laser Vibrometer and the Data Physics Shaker Controller (Ref. 12). This method permits multiple test specimens in a single run, monitors the health of all specimens, and tracks resonances of the specimens, while keeping the stress level (i.e., displacement level) constant. If substantial change in the resonant frequency of any specimen is detected (indicated evolution of damage), the test is automatically stopped and all test data is saved. To accomplish this, synchronized coordination between the two systems was made possible by the developed GCF Test Coordinator, explained in the following paragraphs. Figure 10 depicts a schematic configuration of the closed-loop GCF testing algorithm in which the two systems are connected and coordinated. As shown, one of the important features of the GCF Test Coordinator is synchronization between the two systems with flexible testing time tracked for each specimen. Particularly, this feature allows controlling the speed of scanning over multiple specimens. Operators have the discretion to preset the dwell test duration assigned to each specimen to assure that any abrupt fatigue failure is captured.

5.1 GCF Test Coordinator

Typically, the Polytec SLV system measures each scan point during a single pass (pass meaning one complete scan of all specimens). After a pass, it saves all the data in a single file and stops measuring. However, to run the GCF test until fatigue failure and to continuously monitor the health of specimens, it was required to measure each point multiple times throughout the length of the test. Consequently, a new automation technique was developed that employed the Visual Basic macro engine (Test Automation Object Library) that comes with the PSV system. Using this, it was possible to control and modify the PSV applications programmatically via the built-in macro subsystem. Thus the macro program was

developed to control the PSV system for multiple measurements. The user pre-sets the intended number of passes, and after completing one pass of all the scan points, the measurement system restarts automatically, and this process continues. To facilitate data analysis, a program was also developed to save the pass data separately for each scan point for every measurement cycle.

Macro code was also developed to access the data acquisition settings from the program. Time and frequency domain acquisition parameters, such as sampling frequency or number of samples, were pre-defined within the macro subroutine.

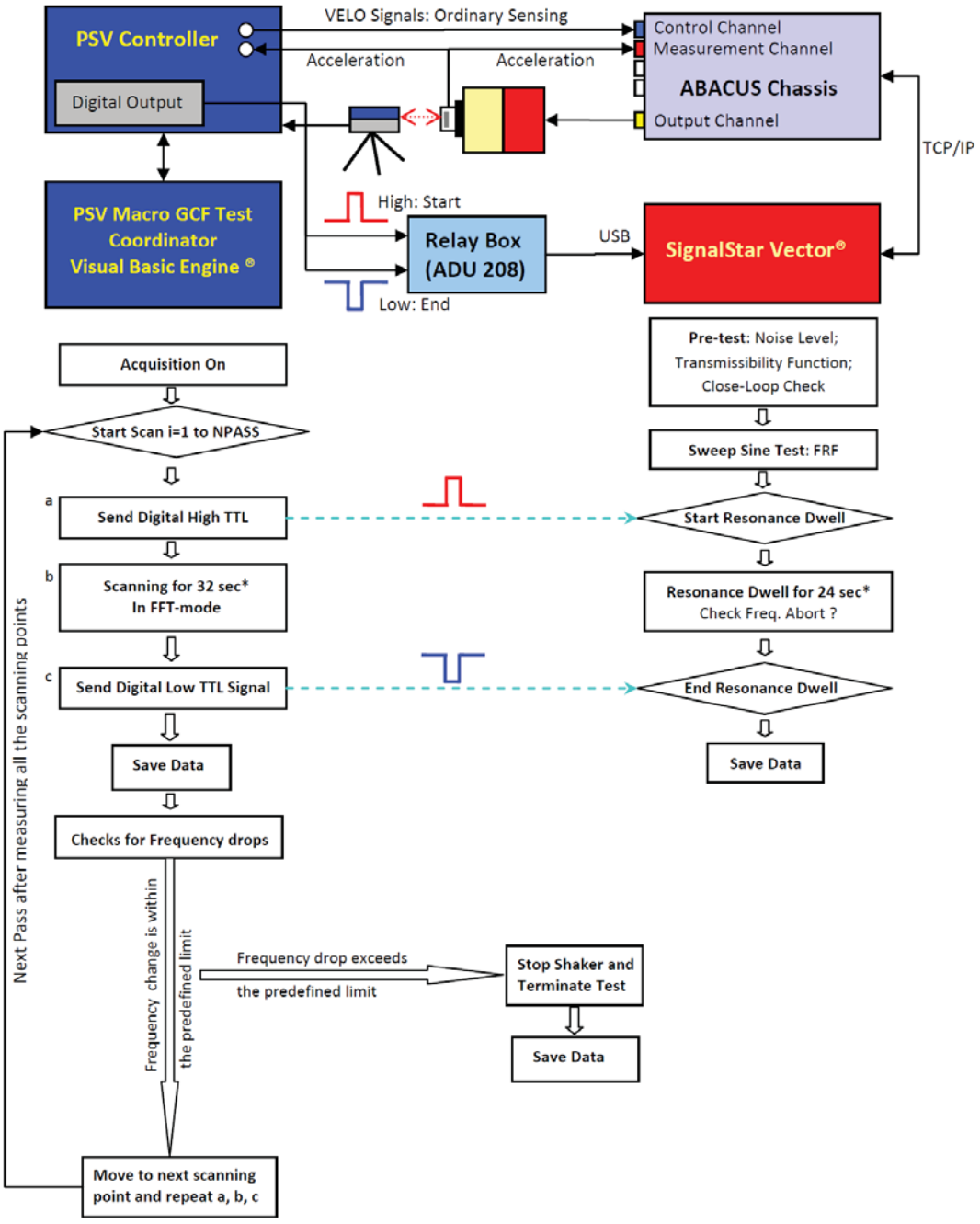

Figure 10.—Closed-loop GCF test control using PSV macros; resonance dwell control algorithm in SignalStar Vector.

Macro programming was used to synchronize the Polytec PSV system with the DP SignalStar Vector Shaker Controller; these communicate by sending digital pulses (TTL) to the digital output port. A DP relay box is used as a communicating device between the two systems. Two different types of digital pulse are generated thru macro code: high level pulse, and low level pulse; these create start and stop signals. The required duration of the pulse was also set in the macro program. When a new measurement is about to start, a start-up pulse is sent to the DP system to generate and control the excitation, and a stopping pulse is sent at the end of measurement. Thus, the macro code repeats starting and stopping the DP resonance dwell test multiple times, with preset time intervals for each of the scanning points.

In frequency measurement mode, the macro was programmed to search for the maximum amplitude in the frequency response function (FRF) spectrum. Subsequently, the corresponding frequency at the maximum spectral amplitude is deemed the resonant frequency, and it is used as a controlling criterion for the closed-loop system. When the frequency drops a preset percentage (for example, 2 to 10 percent) of the previous frequency, the macro code sends a stopping pulse to the DP system to terminate the test.

5.2 DataPhysics SignalStar Vector Software

For closed-loop GCF testing, DataPhysics SignalStar Vector (Data Physics Corporation) (referred as DP Vector software in the following) is used as the shaker controller. The resonance dwell test option in DP Vector software is designed to perform vibration-based fatigue testing by tracking the resonant frequency of a tested specimen. To track resonant frequencies, a sine sweep test needs to be undertaken prior to the dwell test in order to save the frequency response function and phase angle.

Two signal channels are used: one for the control channel, which is fed continuously by velocity signals from PSV system (OFV-5000), and the other for a measurement channel, where acceleration signals are measured by the Dytran accelerometer installed on the shaker armature.

The peak frequency and its corresponding phase angle are selected in the resonance dwell test window. In the dwell test, the phase angle is set to be continuously tracked. This allows a change in shaker driving frequency to the initial resonant frequency of the specimen. Another important feature in DP shaker system is its capability to control the vibration level. Operators can set a targeted displacement, velocity, or acceleration signal level, measured by PSV laser vibrometer. Then the DP software continuously adjusts shaker driving voltages to maintain the preset targeted level.

5.3 Procedures for Closed-Loop GCF Testing

Descriptive procedures for the developed testing methodology steps follow.

Step 1. A pretest should be conducted prior to running any test with the DP shaker system. Its purpose is to check the signal-to-noise ratio and to verify closed-loop control with the control channel (laser vibrometer), the reference channel (accelerometer), and the transfer function. If this pretest is passed, it need not be run again.

Step 2. Sweep sine tests are conducted for each of the 10 specimens installed prior to running closed-loop GCF testing. This evaluates the 10 specimens to assure that they have nearly identical natural frequencies and corresponding phase angles, so that one representative FRF and phase angle can be used for control. To attain the narrowest frequency range between specimens, a precise torque wrench is used to tighten fixture bolts, and specimen lengths are trimmed also as needed. In the near future, it is expected that DP Vector software will be able to accommodate multiple FRFs assigned to multiple resonance dwell tests in the closed-loop GCF testing; DP plans to revise the Vector software to accommodate these special needs for GCF testing.

Step 3. The sweep sine test results, i.e., the FRF and phase angle chart, are assigned to the resonance dwell test.

Step 4. The closed-loop resonance dwell GCF testing is triggered by a start TTL signal from GCF Test Coordinator to the DP system.

Step 5. The PSV scans the first specimen for 32 sec (the scanning interval can be user-modified). In the DP system, a resonance dwell test runs for 24 sec. For smooth restarting, the resonance dwell test should end before the PSV system completes scanning the first specimen. The time difference is set to 8 sec. This time is used for initializing and ending the DP software and for transferring stop and start TTL signals, etc. During the resonance dwell test, frequency or amplitude abort criteria can be turned on to stop the test should these limits be exceeded.

Step 6. The GCF Test Coordinator stores the maximum magnitude of the FRF and its corresponding frequency, which is close to the excitation frequency that is determined by the DP system, and computes the accumulated number of cycles. Test data for each specimen are saved in files on an external hard disk.

Step 7. If the frequency drop for a specimen is found to exceed the preset criterion (for example, 10 Hz), the GCF Test Coordinator sends a stopping pulse to the DP system, and the test is terminated. It is presumed that the stiffness loss is due to fatigue cracking, and this is verified later by optical examination.

Step 8. If the frequency change for the specimen is less than the preset limit, the laser beam moves to next specimen and the GCF Test Coordinator sends a start TTL signal to the DP system. ***Steps 3*** to ***8*** are repeated until the preset frequency drop criterion is exceeded.

6.0 Experimental Testing and Results

6.1 Stress Evaluation

First, a series of simple tension tests on the specimen material were conducted to determine the yield stress level. Stress-strain curves for two samples are shown in Figure 11.

To ensure that the stress level was high enough to induce fatigue cracking in specimens for the given shaker power, specimens with lengths ranging from 139 to 42.5 mm (5.475 to 1.675 in.) were manufactured. Figure 12 shows five of the tested specimen lengths. For the various length specimens, the maximum attainable specimen strains, specimen tip displacements, and shaker armature displacement amplitudes were measured, using the shaker at maximum power. Vishay strain gages (WK-06-062AP-350), the scanning laser vibrometer, and Dytran accelerometer (3030B) were used to measure specimen strains, specimen tip displacements, and armature displacements, respectively. For this test, all 10 specimens were installed in the 10-specimen fixture, which was mounted on the shaker armature as is planned for actual ASC GCF testing. The strain gage lead wires were connected to four hair-like copper wires (two of them were for backup) to minimize any mechanical effects on specimen vibration; they were soldered together using adapters, and then insulated with an enamel coating. A distance away from the specimen, the shielded sensor cables were connected to the NI-DAQ system. The strain gages were installed at the location of maximum stress as predicted by the 3D FE analysis. After successful testing, this location was verified from actual crack locations in failed specimens.

Before running the GCF test, the first bending mode natural frequencies of the test specimens were identified from sine sweep testing using the DP Vector software. As shown in Figure 13, natural frequency of the first mode increased as the length of specimen decreased. (The specimen length was measured from clamped edge to free end excluding the gripped zone.) Natural frequencies ranged from 82 to 1100 Hz. After identifying the natural frequencies, the DP shaker system was operated at its maximum power level and with the excitation frequency tuned to the identified natural frequencies. Shaker driving voltage signals were generated from an external function generator (Agilent Function Generator 33250A). In the test, specimens longer than 100 mm (4 in.) failed within 1 min since the stress levels were very high (over 645 MPa). Because of the short test duration, the tip displacement and armature displacement amplitude could not be measured. Fatigue crack locations for these two cases are shown in Figure 14. As previously mentioned in Section 4.2 (Evaluation of Damping), damping

significantly influences the stress level in 3D FE analyses. It was observed that damping gradually increased as the specimen tip deflection amplitude increased. The source of damping could be a combination of effects from the clamped edge, inherent material damping, hysteretic damping during plastic deformation, air damping, or other damping losses. Due to such uncertainties in predicting damping, the value of damping used for the 3D FE model was based on the experimentally measured strains and corresponding stresses and was modeled as structural damping. Likewise, measured amplitude data for the shaker armature (previously discussed in Section 3.0) at maximum operating power were used in 3D FE analyses.

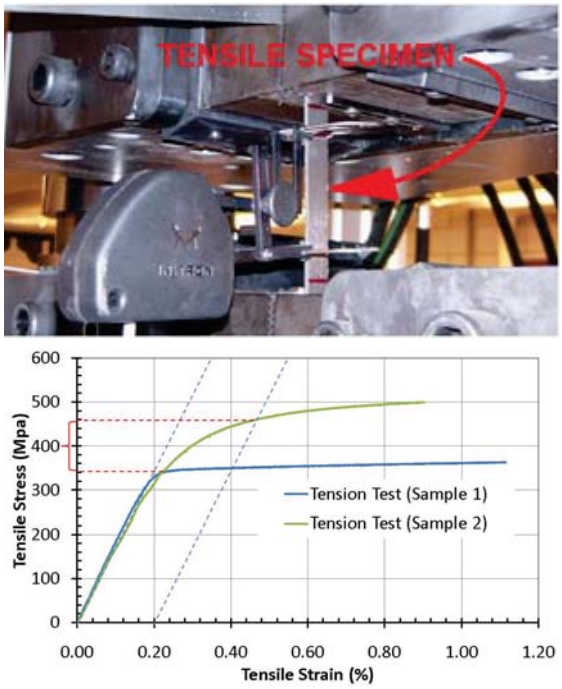

Figure 11.—Simple tension test of specimen material.

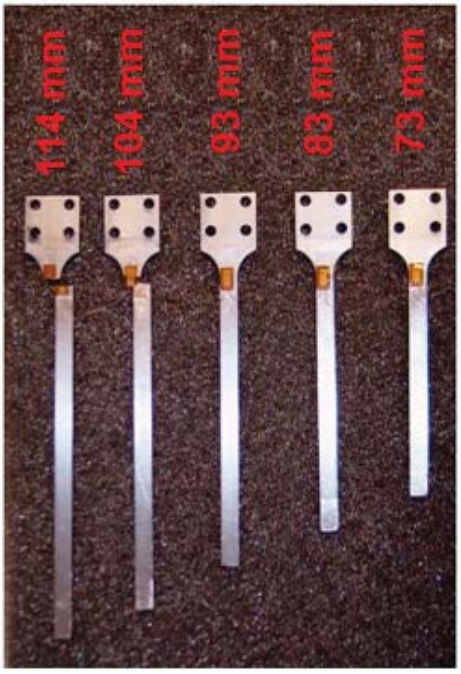

Figure 12.—Five specimens tested for stress evaluation.

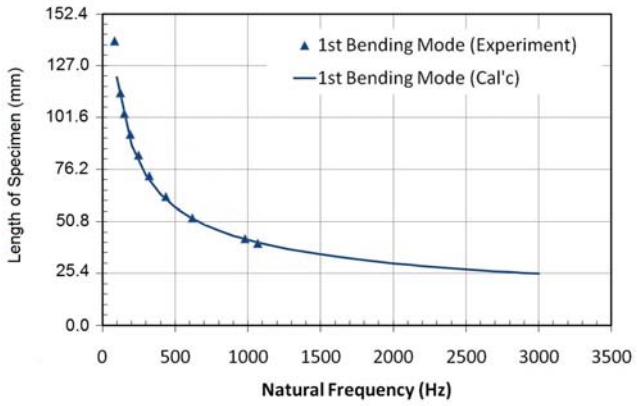

Figure 13.—Specimen lengths and natural frequencies.

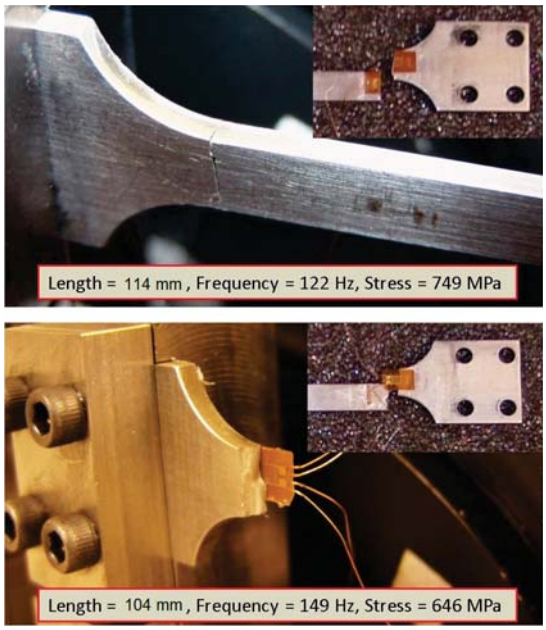

Figure 14.—Fatigue failure and location of crack.

Figures 15 and 16 show correlations between natural frequencies, strains, and stress levels. Note that calculated stresses (749 and 646 MPa, corresponding to failed specimens) at the lower frequencies were overestimated by the employed assumption of linear behavior (Young's modulus = 205,000 MPa) which was not valid for the observed plastic deformation cases.

As shown in Figure 17, the measured tip displacement amplitude gradually decreased as the natural frequency increased. However, at low natural frequencies, the tip amplitudes were overestimated since the natural frequencies were not re-tuned to account for material yielding.

Figure 18 indicates variation of structural damping calculated from the 3D FE analyses. As expected, the damping significantly increased as the natural frequency decreased. As previously mentioned, this may be due to air damping at large tip amplitudes, hysteretic damping due to material yielding, or some other effect.

For a validation test of the closed-loop GCF test method, preliminary stress levels and the resulting specimen lengths were determined from fatigue curves (Stress vs. Number of cycles, or simply, S-N curves) for the AISI 1095 steel specimen material, using data from References 13 and 14 for bending mode fatigue. Yield stress of 350 to 450 MPa was known based on tensile tests previously discussed and shown in Figure 11. With this information, 10 specimens with an initial overall length of 107 mm (4.2 in.) were prepared for the validation test. To demonstrate that the shaker system could precipitate fatigue damage, one test was performed until a specimen failed by high cycle fatigue. A detailed description of the testing is included in the following paragraphs.

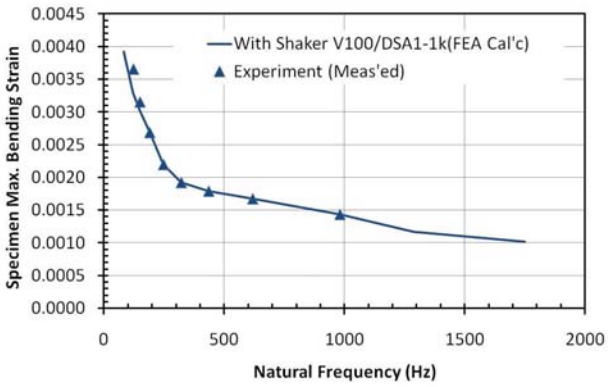

Figure 15.—Max. bending strain vs. natural frequency.

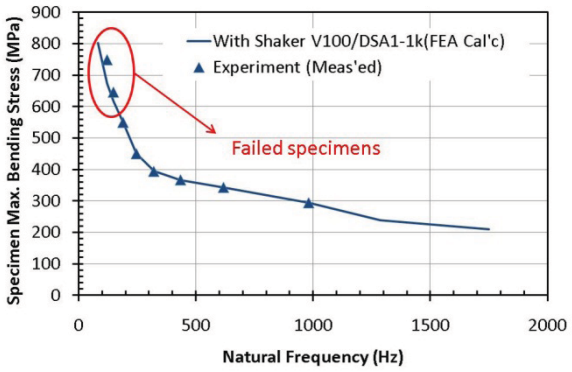

Figure 16.—Max. bending stress vs. natural frequency.

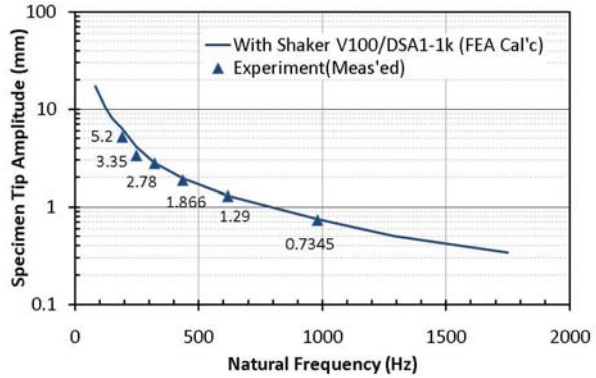

Figure 17.—Tip displacement vs. natural frequency.

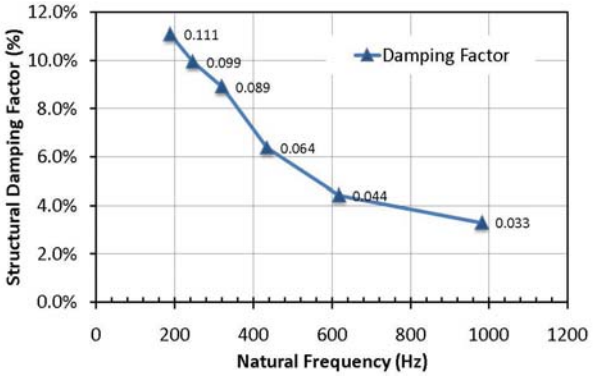

Figure 18.—Damping vs. natural frequency.

6.2 Validation Tests for Closed-Loop GCF Testing

Two validation tests were performed. For the first validation test, a 10^6-cycle experimental fatigue test was conducted. The purpose of this test was to assure that the closed-loop GCF testing could run successfully with the programmed fatigue testing scheme for a 10-specimen configuration (Fig. 19) in coordination with the DP Vector software. At the beginning, sine sweep tests were performed for the now shortened 63.5 mm (2.5 in.) long specimens to obtain FRFs. The first bending mode's natural frequencies and the corresponding phase angles are shown in Figure 20. Reflective film was used at the specimen tips for higher quality velocity signals from the laser.

As seen in the chart, the natural frequencies among the 10 specimens were quite similar. The FRF for Specimen ID 5 was chosen arbitrarily as the reference FRF, which was used for the entire test duration of the resonance dwell test. The maximum tip displacement was set as 0.45 mm (0.018 in.) from zero to peak (0-pk), and this was maintained by the DP shaker controller throughout the test. The stress level at this level of tip amplitude was calculated to be between 250 and 300 MPa. It was found that fatigue failure was not induced in the specimens at this stress level within the desired cycle range. However, the test did demonstrate validity of the developed GCF test methodology. At the 9th pass, it was decided to alter the test by attaching a weight to Specimen ID 10 (only), simulating crack growth by lower its natural frequency below the threshold level.

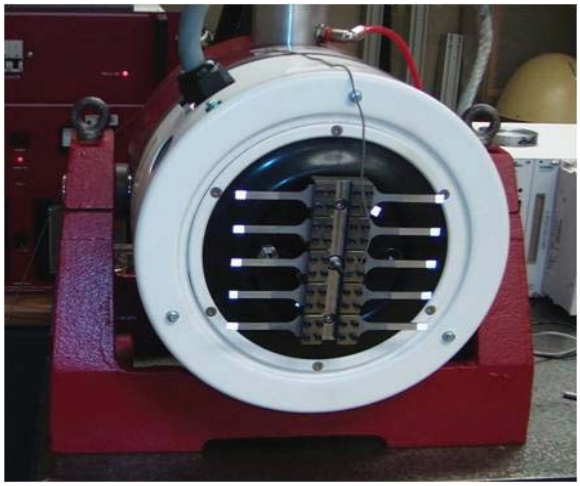

Figure 19.—Ten specimens mounted on armature.

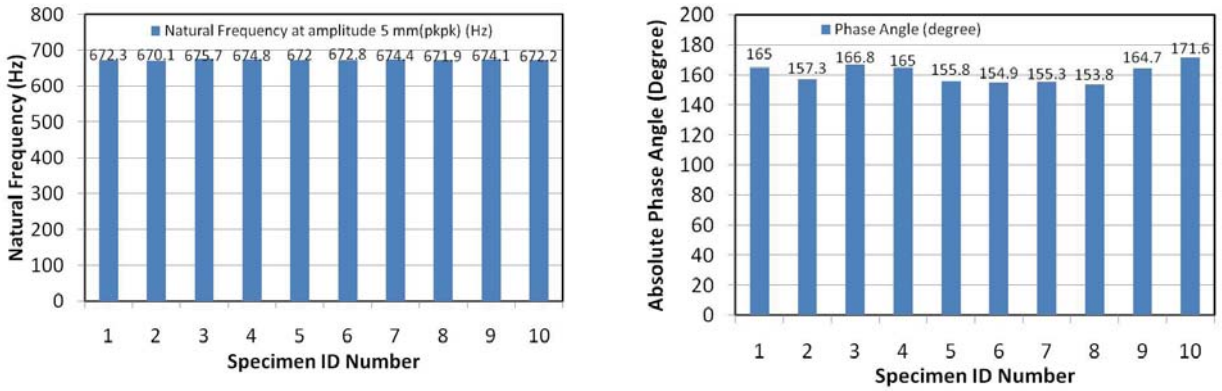

Figure 20.—Frequencies and phase angles of 10 specimens.

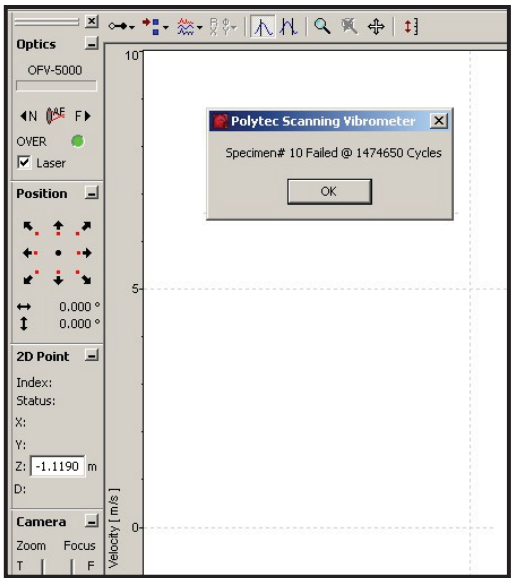

Figure 21.—Pop-up showing detection of fatigue failure.

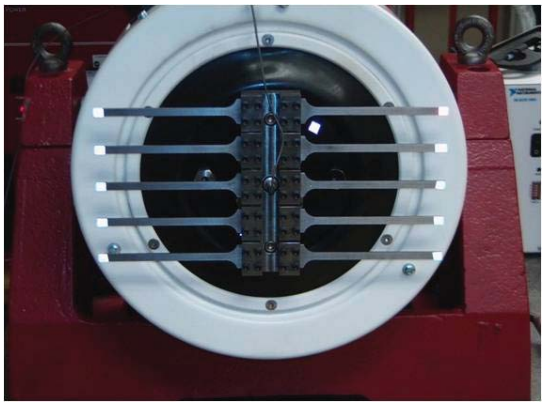

Figure 22.—Ten long specimens on armature.

In the GCF Test Coordinator, the number of passes was set to an arbitrarily large number to enable a long test duration. A frequency drop of 10 Hz below the previous measurement was set as the test abort criterion. Smooth running of the closed-loop method was observed during the experiment. The GCF Test Coordinator sent a starting pulse before the commencement of each measurement and a stopping pulse at the end. After measurement of all the specimens, it went back to the first specimen and started the next pass. Finally, at the end of that 9^{th} pass and after completing over 10^6 fully reversed bending cycles, the GCF Test Coordinator successfully stopped the shaker test after measuring the frequency drop triggered by the weight-simulated fatigue crack initiation. Figure 21 shows the pop-up message which names the specimen ID and total number of accumulated cycles.

Appendix B, Figure 31 shows the data saved by the GCF Test Coordinator, which for each specimen includes: specimen ID, number of measurement passes, measured natural frequency, FRF magnitude, and accumulated number of completed cycles.

The resonance dwell test was repeated to validate the test abort operation upon fatigue failure detection for a revised test procedure. For this case, the DP Vector software was set to abort the test upon breach of the frequency upper and lower bounds set at ±10 percent of the resonance frequency. (This abort option in DP Vector was turned off during the first validation test, as the criterion was set in macro code.)

For this test, specimens were 93.3 mm (3.675 in.) long (Fig. 22); including the clamped region, the end-to-end length was 107 mm (4.2 in.). Stress analysis indicated a maximum stress of 550 MPa for a tip displacement amplitude of 5.2 mm (0.205 in.) 0-pk using maximum shaker power. The specimen's first bending mode was calculated as 190 Hz; Figure 23 shows the measured natural frequencies and phase angles for the 10 specimens.

The test was initiated using the planned 550 MPa stress level, but being over the yield point caused rapid specimen failure. To reach longer fatigue lives, the tip displacement amplitude was reduced to less than 5.0 mm. Figure 24 shows the resulting velocity amplitude and excitation frequency as measured by the laser vibrometer. As evident, the velocity amplitudes displayed high signal noise after 100 sec, which indicated the formation and propagation of fatigue cracking in the specimen. The frequency dropped at a higher rate after 140 sec. This result was coincident with velocity amplitude, which also dropped synchronously. On the contrary, tracking of phase angle proved to be less discriminatory, as shown in Figure 25; the resonance dwell test tracked the phase angle (173°) that was assigned prior to the testing, but changed little, even during crack initiation and growth. After automated termination of the test, the specimen was visually inspected, and the fatigue crack seen in Figure 26 was discovered.

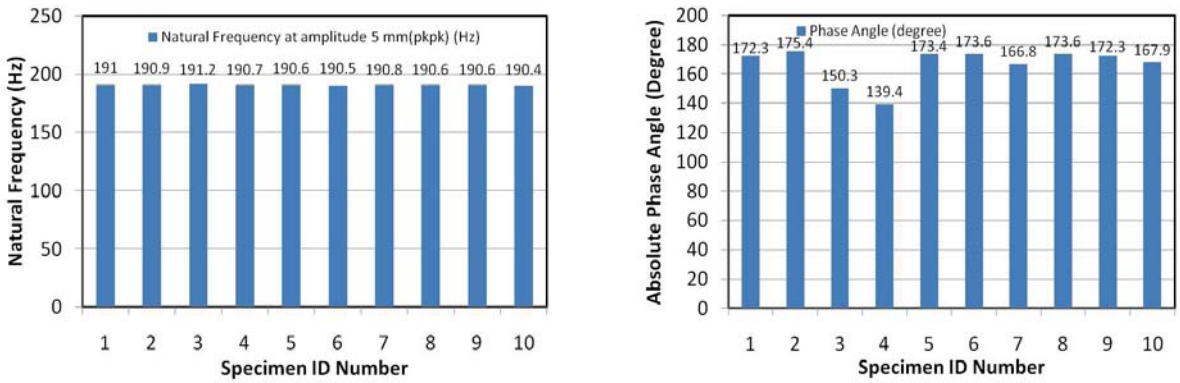

Figure 23.—Natural frequencies and phase angles.

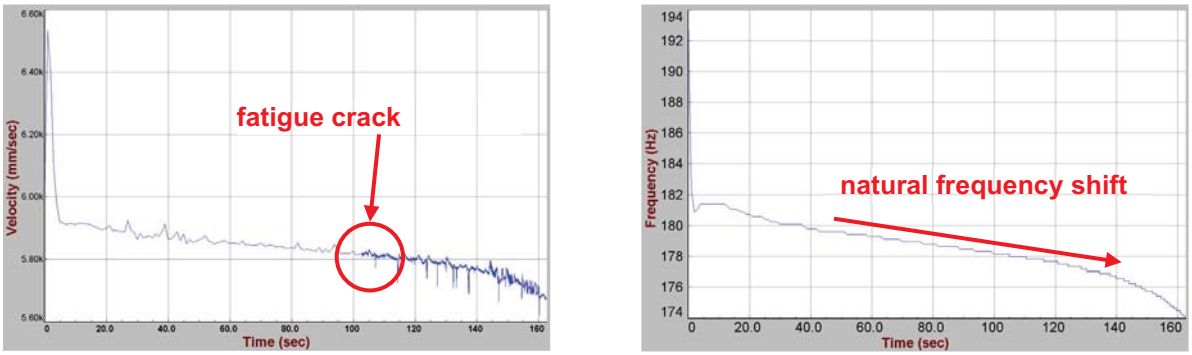

(a) (b)

Figure 24.—(a) Velocity and (b) frequency measured by laser vibrometer; changes due to fatigue cracking.

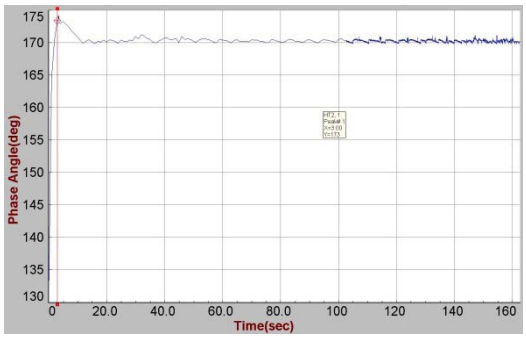

Figure 25.—Phase angle tracking.

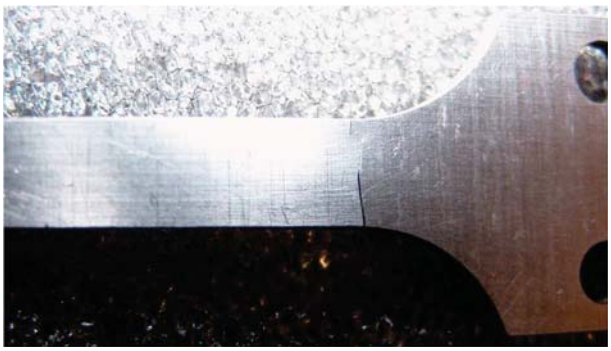

Figure 26.—Fatigue crack in specimen after test.

7.0 Summary

A test procedure and necessary instrumentation to acquire valid experimental data was developed and verified for giga-cycle fatigue testing. Required control over test operation and automated abort was attained with the described GCF Test Coordinator, which managed the equipment involved. At various stages of the effort, the shaker was evaluated to check adequacy of power to reach the targeted stress levels in test specimens at various excitation frequencies. Several specimen and fixture geometries were tested to obtain a design that optimized the excitation frequency, test time, and attainable stress levels in the test specimens. Damping evaluation was carried out by measuring the experimental response from specimens of various lengths to known excitation inputs, and then iterating the value of structural damping in finite element analyses to produce the equivalent calculated response. Experimental strain measurements as well as calibration testing were conducted to obtain relationships between the specimen peak tip displacements and maximum stresses.

The multi-specimen closed-loop testing methodology was verified by preliminary experiments that confirmed the feasibility and applicability of the technique. It was shown that this vibration-based automated method was able to detect the presence of fatigue cracking in test specimens while the crack was still in the early stages of propagation, through observed changes in the specimen's resonant frequency; thus, testing can be terminated to prevent further damage if desired. The development of this technique was an important step in obtaining very high cycle count bending fatigue data. The next step will be to use this novel testing methodology to study and control fatigue crack propagation in specimens fabricated from the Advanced Stirling Convertor's Displacer Spring material.

Appendix A.—Detailed Drawings for Giga-Cycle Fatigue Specimen and 10-Specimen Fixture

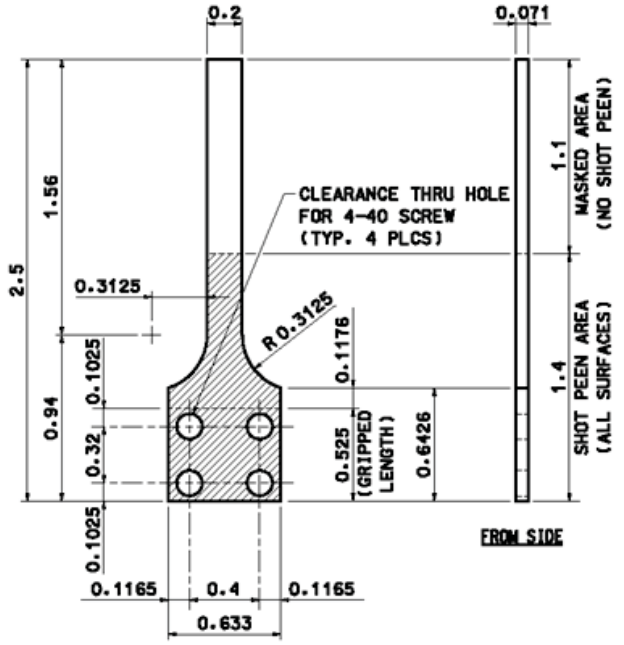

Figure 27.—Drawing of 64 mm (2.5 in.) long specimen (all dimensions shown in inches).

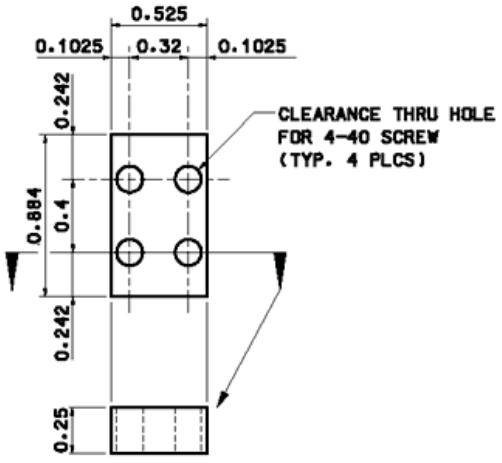

Figure 28.—Drawing of upper block for 10-specimen fixture (all dimensions shown in inches).

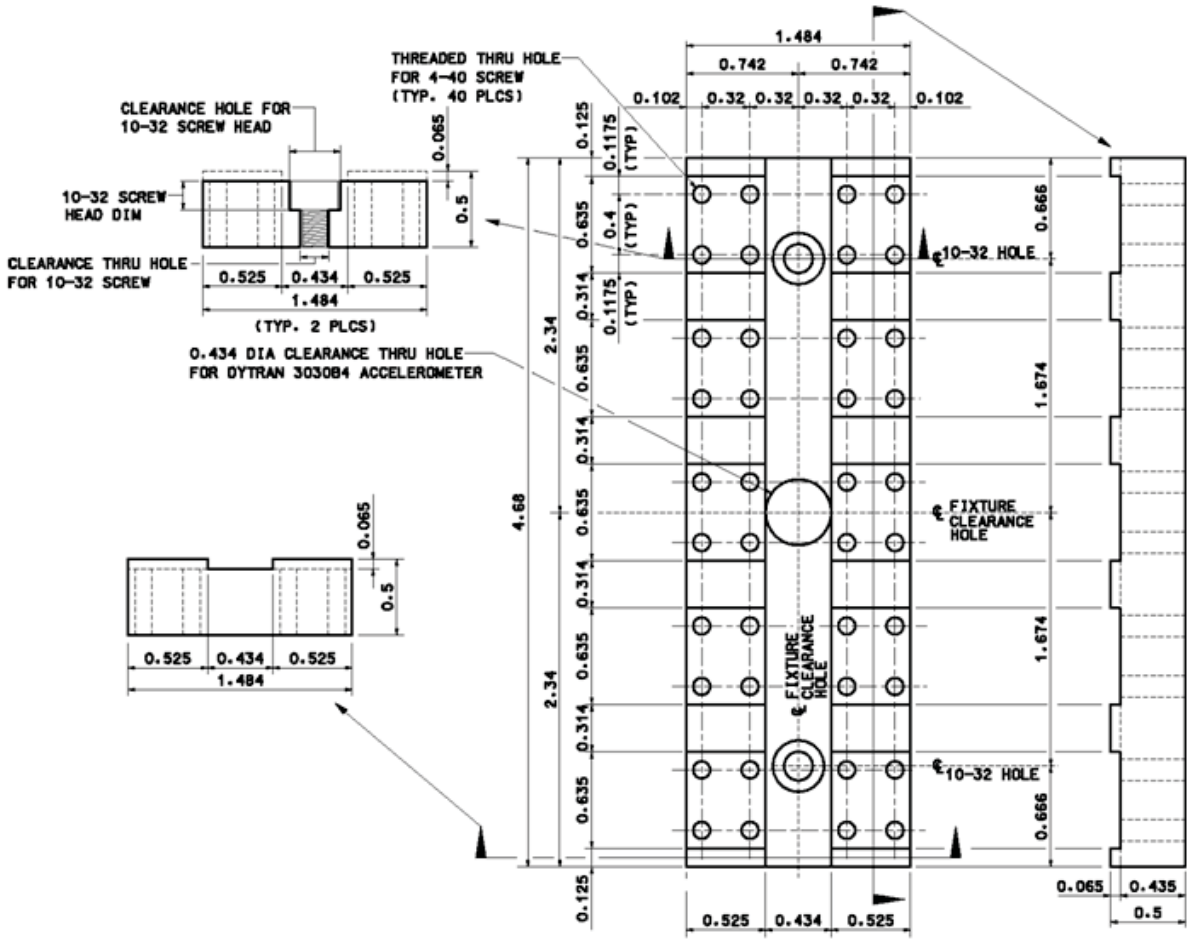

Figure 29.—Drawing of lower block for 10-specimen fixture (all dimensions shown in inches).

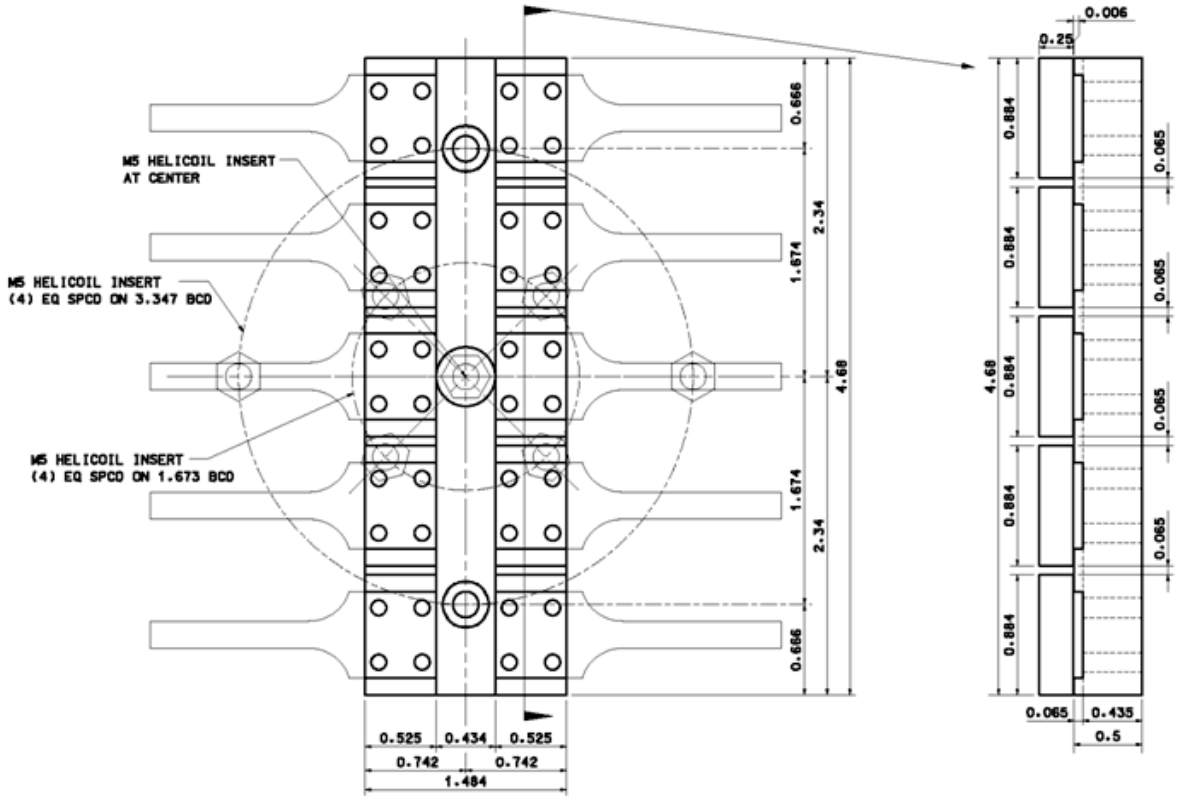

Figure 30.—Ten-specimen fixture arrangement on shaker armature (all dimensions shown in inches).

Appendix B.—Data Saved by the GCF Test Coordinator

Sp_01.txt - Notepad

File Edit Format View Help

(Pass)	(Sp01-freq [Hz])	(Sp01-mag [dB])	(Cycles)
00000001	00666.88	-00027.69	000000016005
00000002	00670.00	-00026.28	000000176880
00000003	00670.00	-00025.33	000000337260
00000004	00672.50	-00026.03	000000497790
00000005	00670.62	-00026.28	000000658050
00000006	00670.00	-00024.21	000000818130
00000007	00668.75	-00029.04	000001010100
00000008	00670.00	-00025.16	000001170570
00000009	00672.50	-00025.84	000001330920

Sp_02.txt - Notepad

File Edit Format View Help

(Pass)	(Sp02-freq [Hz])	(Sp02-mag [dB])	(Cycles)
00000001	00669.38	-00028.76	000000032070
00000002	00666.25	-00028.56	000000192870
00000003	00666.88	-00025.80	000000353265
00000004	00669.38	-00028.74	000000513855
00000005	00666.25	-00027.04	000000674040
00000006	00658.12	-00027.62	000000833925
00000007	00666.88	-00024.28	000000977970
00000008	00669.38	-00028.82	000001026165
00000009	00671.88	-00022.34	000001186695

Sp_03.txt - Notepad

File Edit Format View Help

(Pass)	(Sp03-freq [Hz])	(Sp03-mag [dB])	(Cycles)
00000001	00666.88	-00018.10	000000048075
00000002	00662.50	-00029.17	000000208770
00000003	00665.62	-00029.51	000000369240
00000004	00661.88	-00025.61	000000529740
00000005	00656.88	-00026.21	000000689805
00000006	00655.00	-00027.76	000000849645
00000007	00655.62	-00027.32	000001041900
00000008	00661.88	-00025.09	000001202580
00000009	00665.00	-00029.53	000001362945

Sp_04.txt - Notepad

File Edit Format View Help

(Pass)	(Sp04-freq [Hz])	(Sp04-mag [dB])	(Cycles)
00000001	00673.12	-00030.68	000000064230
00000002	00670.62	-00030.78	000000224865
00000003	00670.00	-00030.41	000000385320
00000004	00669.38	-00031.12	000000545805
00000005	00663.75	-00031.07	000000705735
00000006	00669.38	-00031.53	000000865710
00000007	00670.00	-00030.40	000001057980
00000008	00662.50	-00029.79	000001218480
00000009	00660.62	-00030.87	000001378800

Figure 31.—Data saved by the GCF test coordinator.

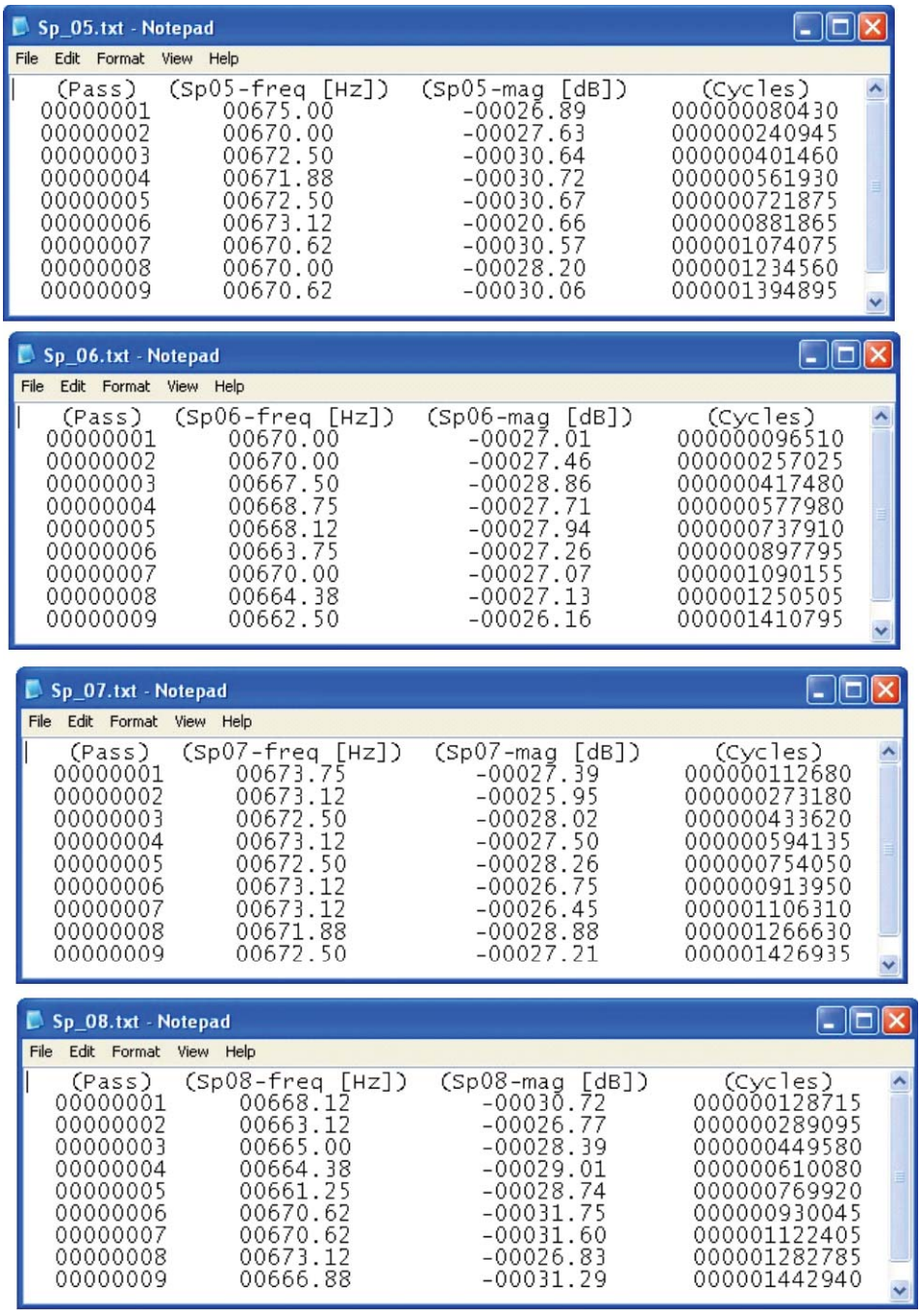

Sp_05.txt - Notepad

File Edit Format View Help

(Pass)	(Sp05-freq [Hz])	(Sp05-mag [dB])	(Cycles)
00000001	00675.00	-00026.89	000000080430
00000002	00670.00	-00027.63	000000240945
00000003	00672.50	-00030.64	000000401460
00000004	00671.88	-00030.72	000000561930
00000005	00672.50	-00030.67	000000721875
00000006	00673.12	-00020.66	000000881865
00000007	00670.62	-00030.57	000001074075
00000008	00670.00	-00028.20	000001234560
00000009	00670.62	-00030.06	000001394895

Sp_06.txt - Notepad

File Edit Format View Help

(Pass)	(Sp06-freq [Hz])	(Sp06-mag [dB])	(Cycles)
00000001	00670.00	-00027.01	000000096510
00000002	00670.00	-00027.46	000000257025
00000003	00667.50	-00028.86	000000417480
00000004	00668.75	-00027.71	000000577980
00000005	00668.12	-00027.94	000000737910
00000006	00663.75	-00027.26	000000897795
00000007	00670.00	-00027.07	000001090155
00000008	00664.38	-00027.13	000001250505
00000009	00662.50	-00026.16	000001410795

Sp_07.txt - Notepad

File Edit Format View Help

(Pass)	(Sp07-freq [Hz])	(Sp07-mag [dB])	(Cycles)
00000001	00673.75	-00027.39	000000112680
00000002	00673.12	-00025.95	000000273180
00000003	00672.50	-00028.02	000000433620
00000004	00673.12	-00027.50	000000594135
00000005	00672.50	-00028.26	000000754050
00000006	00673.12	-00026.75	000000913950
00000007	00673.12	-00026.45	000001106310
00000008	00671.88	-00028.88	000001266630
00000009	00672.50	-00027.21	000001426935

Sp_08.txt - Notepad

File Edit Format View Help

(Pass)	(Sp08-freq [Hz])	(Sp08-mag [dB])	(Cycles)
00000001	00668.12	-00030.72	000000128715
00000002	00663.12	-00026.77	000000289095
00000003	00665.00	-00028.39	000000449580
00000004	00664.38	-00029.01	000000610080
00000005	00661.25	-00028.74	000000769920
00000006	00670.62	-00031.75	000000930045
00000007	00670.62	-00031.60	000001122405
00000008	00673.12	-00026.83	000001282785
00000009	00666.88	-00031.29	000001442940

Figure 31.—Continued.

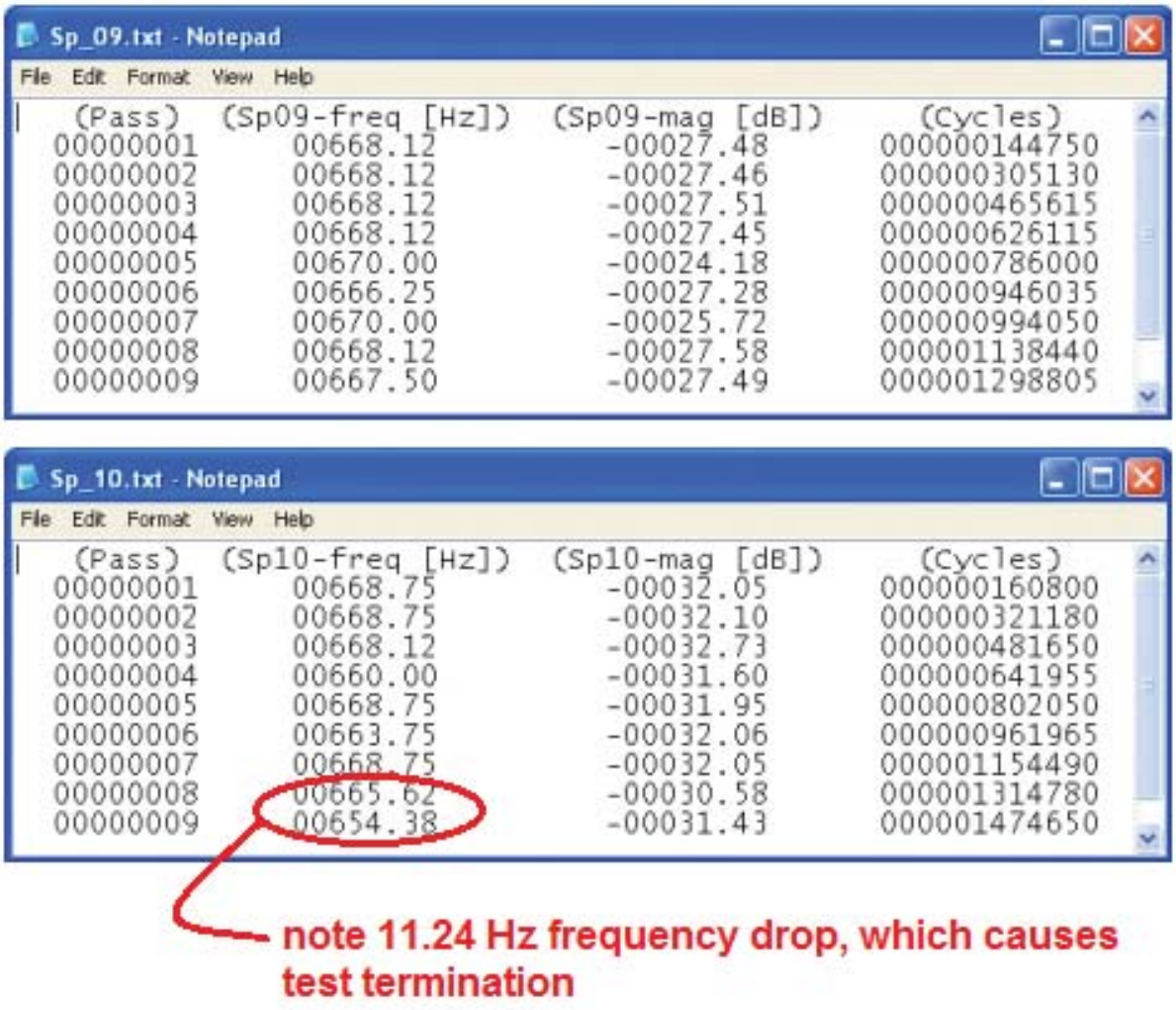

Figure 31.—Concluded.

References

1. Wong, Wayne A.; Wood, J. Gary; and Wilson, Kyle: Advanced Stirling Convertor (ASC) - From Technology Development to Future Flight Product. NASA/TM—2008-215282, 2008.
2. Schreiber, Jeffrey G.; and Thieme, Lanny G.: GRC Supporting Technology for NASA's Advanced Stirling Radioisotope Generator (ASRG). Space Technology and Applications International Forum (STAIF-2008), edited by M.S. El-Genk, AIP Conference Proceedings 969, Melville, New York, 2008, pp. 582–592.
3. Shaltens, Richard K.; and Wong, Wayne A.: Advanced Stirling Technology Development at NASA Glenn Research Center. NASA/TM—2007-214930, 2007.
4. Object Model Reference, Visual Basic® Engine, PSV 8.3. Polytec, Inc.
5. Vibrometer Controller User Manual, OFV-5000. Polytec, Inc.
6. Polytec Scanning Vibrometer Software Manual, Software 8.2. Polytec, Inc.
7. Polytec Scanning Vibrometer Hardware Manual, PSV 400. Polytec, Inc.
8. SignalStar Vibration Controller User Manual, Rev. 09. Data Physics Corp.
9. Data sheet for V100 Shaker. Data Physics Corp.
10. Performance Specification for Series 3030B Accelerometer. Dytran Instruments, Inc.
11. Instruction for Strain Gage Installation. Vishay Micro-measurements.
12. Yun, G.J., Abdullah, A.B.M., and Binienda, W.: Development of a Closed-Loop High-Cycle Resonant Fatigue Testing System. Experimental Mechanics, vol. 52, no. 3, 2011, pp. 275–289.
13. Lee, Yung-Li, Pan, Jwo, Hathaway, Richard, and Barkey, Mark: Fatigue Testing and Analysis: Theory and Practice. Elsevier Inc., Burlington, MA, 2005.
14. Zettle, B., Mayer, H., Ede, C., and Stanzl-Tschegg, S.: Very High Cycle Fatigue of Normalized Carbon Steel. International Journal of Fatigue, vol. 28, no. 11, 2006, pp. 1583–1589.